

# Errata for *Emitter Detection and Geolocation for Electronic Warfare*

Nicholas A. O'Donoughue

April 28, 2025

1. On page 42, Figure 3.8, the min detectable signal level is plotted as -132 dBW, while the text references -142 dBW. This is due to a discrepancy in the assumed channel bandwidth (a bandwidth of 2 MHz leads to -132 dBW, but the example calls for a channel bandwidth of 200 kHz). The corrected figure is below.

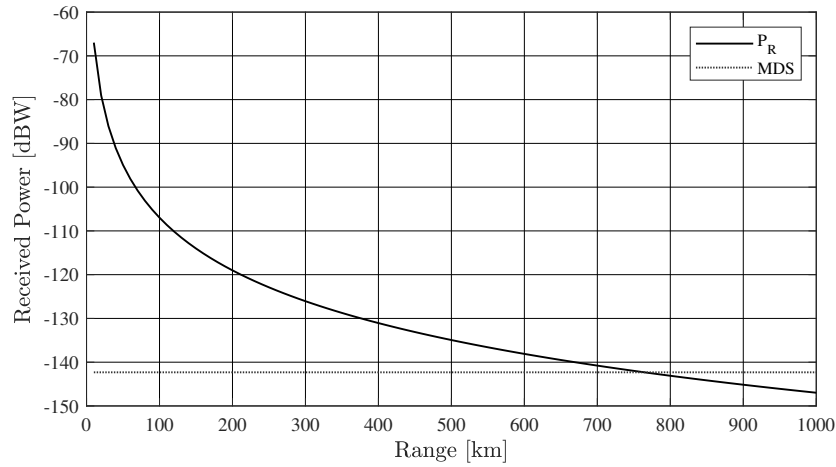


Figure 3.8: Received power (solid line) and minimum detectable signal (dotted line) as calculated in (3.38) with parameters from Section 3.4.2.

2. On page 43, following equation (3.38), the stated detection range is approximately 430 km, based on the erroneous Figure 3.8. The true detection range is approximated with 730, based on the corrected Figure 3.8 above. Further down, the true detection range is calculated and reported as 429.88 km, but the correct result is 764.44 km. The same error is present in Figure 3.9. The corrected figure is below.

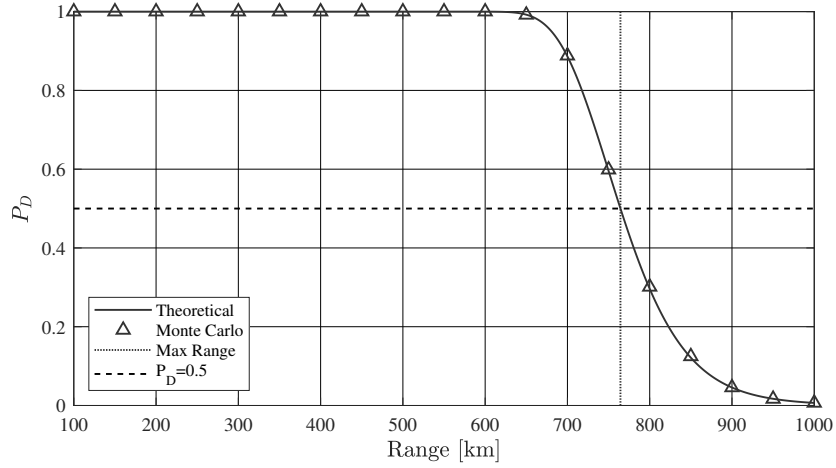


Figure 3.9: Monte Carlo trial plotting probability of detection for an FM tower at various standoff ranges from an ideal receiver, with  $10^5$  trials at each range.

3. On page 45, Table 3.1 referenced an incorrect assumption for the transmit power in the sidelobes. The text and example used  $G_t = 10$  dBi, but the table references  $G_t = 19$  dBi. The corrected table is below.

Table 3.1: Collision Avoidance Radar Parameters for Example 3.2

(a) CA Radar Transmitter		(b) Receiver	
Parameter	Value	Parameter	Value
$P_t$	35 mW	$G_r$	10 dBi
$G_t$ (mainlobe)	34 dBi	$L_r$	2 dB
$G_t$ (sidelobe)	9 dBi	$F_n$	4 dB
$B_s$	31.3 MHz	$B_n$	40 MHz
$f_0$	35 GHz	$h_r$	500m
$L_t$	0 dB		
$h_t$	500m		

4. On page 63, Figure 4.6 has incorrect callouts. They state that  $\xi = 10, 20$ , or 30 dB for the three sets of curves, but they should be calling out the time-bandwidth product, and not the SNR. The corrected figure is below.

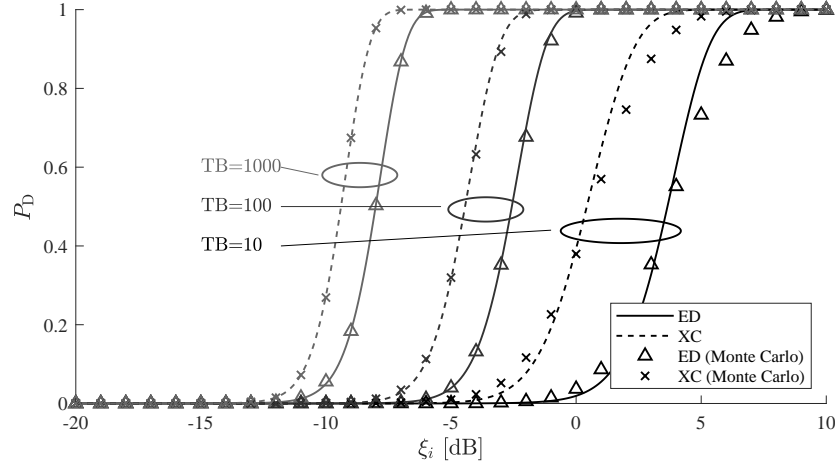


Figure 4.6: Performance comparison of an energy detector (solid lines, triangular marks) and cross-correlation detector (dashed lines, x marks), for various time-bandwidth products.

5. *On page 66, the pulse duration is listed as 20  $\mu$ s, but the figure was generated using 20 ms. The software repository has been updated, and the revised section of text is below, which includes a brief discussion of what to do when the correlation window is longer than the pulse duration.*

We follow a similar approach with the radar pulse as was done with the communications pulse, with one important distinction. Since the correlation window  $T_{corr}$  is larger than the pulse duration  $T_p$ , we must compute the loss due to noise-only samples. For simplicity, we will assume that the entire pulse duration falls within the correlation window (rather than the correlation window beginning part-way through the pulse). This timing loss is computed:

$$L_\tau = \min \left( 1, \frac{T_p}{T_{corr}} \right). \quad (4.30)$$

First the detection thresholds for the energy detector and cross-correlation detector are computed

```
> xi_min_ed = detector.squareLawMinSNR(PFA,PD,M);
> xi_xc = detector.xcorrMinSNR(PFA,PD,Tcorr,Tp,Bn,Bs);
```

The result is  $\xi = -15.98$  dB for the energy detector and  $\xi = -29.49$  dB for the cross correlation detector, a gain of 13.5 dB. Next, we compute the received SNR as a function of range, plotted in Figure 4.8 for mainlobe detection, near-in sidelobe detection, and distant sidelobe detection.

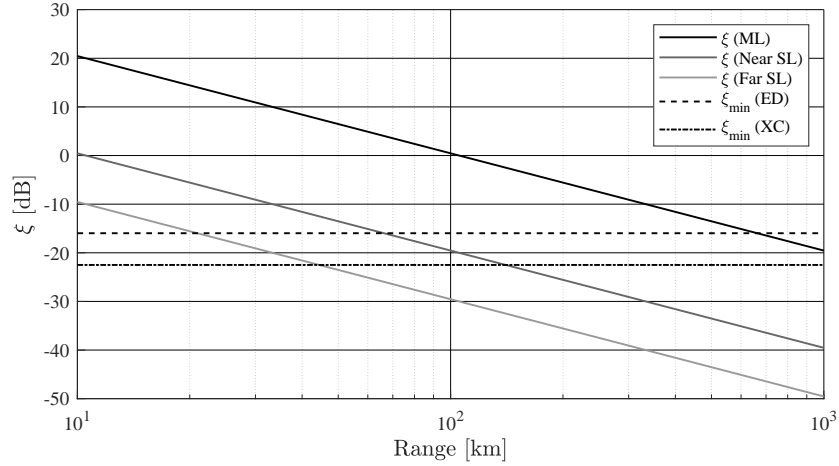


Figure 4.8: Plot of the received SNR as a function of range for the example radar pulse and detector in Example 4.1, compared with the SNR thresholds for the energy detector and cross-correlation detector.

From Figure 4.8, we can see that the energy detector can observe the radar pulse at a range of 663 km (mainlobe), 66 km (near sidelobes), and 21 km (far sidelobes). The cross-correlation detector can extend those maximum ranges to 1,405 km, 140 km, and 44 km, respectively.

6. *On page 75, in the second to last paragraph, the wrong hop rates are reported for the dashed and dotted lines in Figure 5.4, furthermore the variable  $T_{\text{hop}}$  was used when values for  $f_{\text{hop}}$  were provided. The correct text should read:*

If, instead, the signal hops at a rate of  $f_{\text{hop}}=1,000$  hops/sec (dashed line) or 10,000 hops/sec (dotted line), as some modern military datalinks do, similar detection performance would require SNR levels of  $\xi \geq -1.8$  dB or 4.7 dB, respectively.

*The figure in the book is correct, but is replicated here for convenience.*

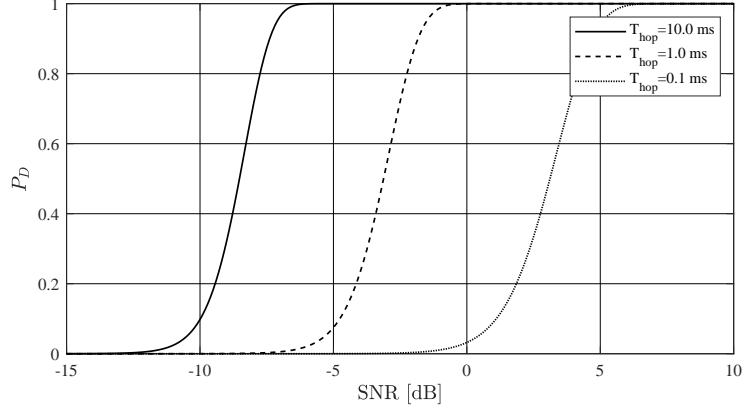


Figure 5.4: Performance of a scanning IF receiver as described in Example 5.1.

7. On page 96, equation (6.38) has a typographical error. The first equivalent is missing a factor  $M$  from the numerator. It should read:

$$= \frac{M}{(\sigma_n^2)^2} \sigma_n^2 = \frac{M}{\sigma_n^2} \quad (6.38)$$

8. On page 99, equation (6.53) and (6.54) have a typographical error, they should read:

$$[\mathbf{F}_{\boldsymbol{\vartheta}}(\mathbf{x})]_{ij} = \frac{1}{2} \text{Tr} \left[ \mathbf{C}^{-1} \frac{\partial C}{\partial \theta_i} \mathbf{C}^{-1} \frac{\partial C}{\partial \theta_j} \right] + \left( \frac{\partial \boldsymbol{\mu}}{\partial \theta_i} \right)^T \mathbf{C}^{-1} \left( \frac{\partial \boldsymbol{\mu}}{\partial \theta_j} \right) \quad (6.53)$$

$$[\mathbf{F}_{\boldsymbol{\vartheta}}(\mathbf{x})]_{ij} = \text{Tr} \left[ \mathbf{C}^{-1} \frac{\partial C}{\partial \theta_i} \mathbf{C}^{-1} \frac{\partial C}{\partial \theta_j} \right] + 2\Re \left\{ \left( \frac{\partial \boldsymbol{\mu}}{\partial \theta_i} \right)^H \mathbf{C}^{-1} \left( \frac{\partial \boldsymbol{\mu}}{\partial \theta_j} \right) \right\} \quad (6.54)$$

9. On page 102, example 6.6 begins with a CRLB stated in terms of the standard deviation, but the CRLB should be defined in terms of error variance. To avoid this confusion, equation 6.62 should be explicitly defined in terms of the standard deviation  $\sigma_\phi$ , and explicitly state that the units of  $\phi$  in this example are degrees. The revised equation 6.62 should read:

$$\sigma_\theta \leq 57.3 \frac{\lambda}{D} \cos \phi \quad [deg] \quad (6.62)$$

Similarly, equation 6.62 should be revised:

$$\sigma_\theta \leq 57.3 \frac{\cos(30)}{10} = 6.62^\circ \quad (6.63)$$

10. On page 103, Problem 6.1 has a typographical error in the PDF. The PDF should be:

$$f(\mathbf{x}|\lambda) = \lambda^{-N} e^{-\lambda \sum_{n=0}^{N-1} x_n}$$

As a result of this change, the variance for which the student is asked to find a maximum likelihood estimate is:  $\vartheta = 1/\lambda^2$

11. On page 112, equation (7.27) provides a small-angle approximation for the gain of an Adcock antenna, and the preceding text claims this is valid for  $d/\lambda \leq .25$ . Under these conditions, the argument to the sin term in (7.26) is bounded by  $[-\pi/4, \pi/4]$ . However, the small-angle approximation ( $\sin(x) \approx x$ ) provides an error of almost 10 % at the extreme of that interval. Consider the following chart:

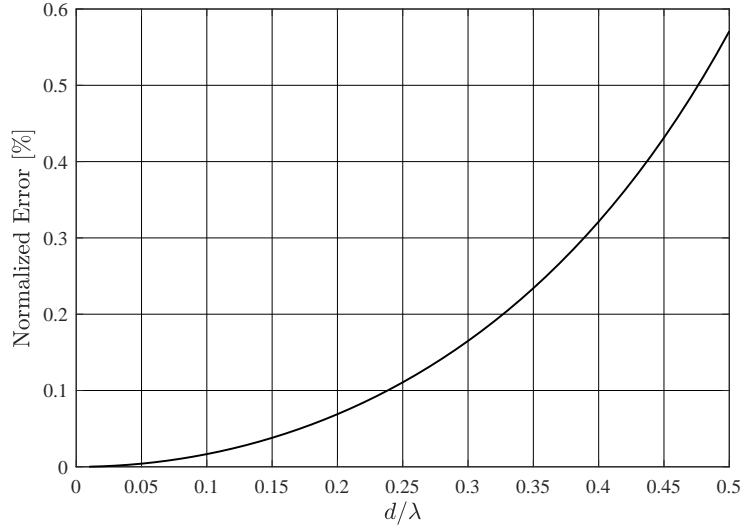


Figure 5.4: Calculation of the percent error for a small-angle approximation of equation (7.26), as a function of  $d/\lambda$ .

As such, the recommendation to apply the small angle approximation of (7.26) should only apply for  $d/\lambda \leq 0.08$ , which leads to an approximation error no greater than 1.06%.

In response to this reduced valid approximation interval, the equations (7.28) and (7.29), should use the unapproximated form:

$$G(\psi) = 2 \sin \left( \pi \frac{d}{\lambda} \cos(\psi) \right) \quad (7.28)$$

$$\dot{G}(\psi) = -2\pi \frac{d}{\lambda} \sin(\psi) \cos \left( \pi \frac{d}{\lambda} \cos(\psi) \right) \quad (7.29)$$

This carries through to equations (7.30-7.32):

$$\mathbf{g}^T \mathbf{g} = 4 \sum_{m=0}^{M-1} \sin^2 \left( \pi \frac{d}{\lambda} \cos(\psi_i - \psi) \right) \quad (7.30)$$

$$\dot{\mathbf{g}}^T \mathbf{g} = \frac{-2\pi d}{\lambda} \sum_{m=0}^{M-1} \sin \left( 2\pi \frac{d}{\lambda} \cos(\psi_i - \psi) \right) \sin(\psi_i - \psi) \quad (7.31)$$

$$\dot{\mathbf{g}}^T \dot{\mathbf{g}} = \left( \frac{2\pi d}{\lambda} \right)^2 \sum_{m=0}^{M-1} \cos^2 \left( \pi \frac{d}{\lambda} \cos(\psi_i - \psi) \right) \sin^2(\psi - \psi_i) \quad (7.32)$$

The code contained in `aoa.make_gain_functions` that was used to generate Figures 7.3 and 7.14 was already using the accurate version of (7.28) and (7.29), rather than the small-angle approximation, so these changes do not invalidate those figures or the results they discussed.

12. An unrelated error in the code for Figure 7.3 did cause a slight error in the computed CRLB. The function `aoa.make_gain_functions` contained a `cosd` instead of a `cos` in one location, causing an increase in the reported CRLB. This was matched with an noise power calculation error in the matching Monte-Carlo simulation that caused a 3 dB increase in noise power. The corrected figure is shown below:

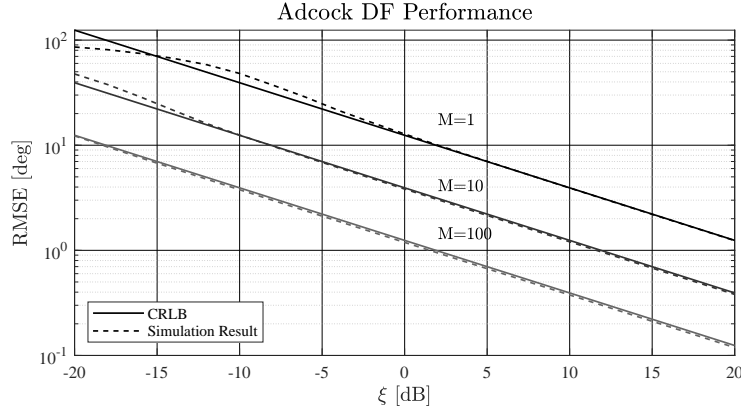


Figure 7.3: Illustration of CRLB performance for an amplitude-based DOA with an Adcock antenna, compared with results from a Monte Carlo trial.

13. On page 155, figure 8.6 has a typographical error, the y-axis label should reference [dB] not [linear] for the units. The corrected graphic is:

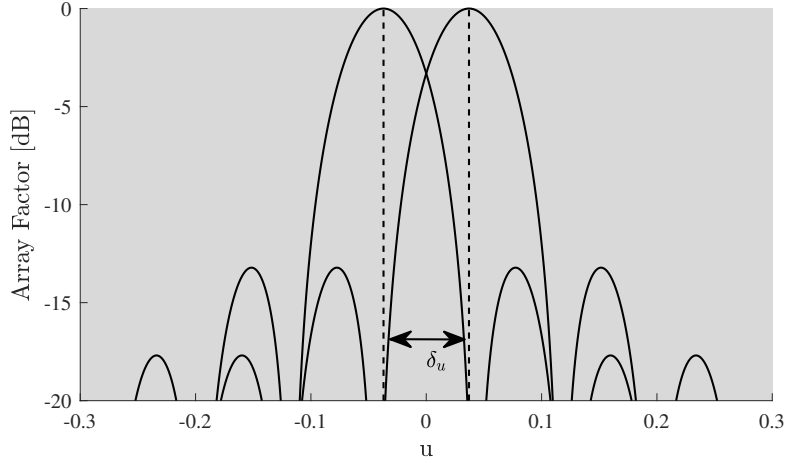


Figure 8.6: Array factor for a standard beamformer responding to two signals separated by the array beamwidth.

14. On page 161, equation (8.41) has a typographical error, there is a missing ‘-’ in the summation term. The equation should read:

$$\ell(\mathbf{x}|\boldsymbol{\psi}, \mathbf{s}) = -MN \ln \sigma_n^2 - \frac{1}{\sigma_n^2} \sum_{m=0}^{M-1} |\mathbf{x}[m] - \mathbf{V}\mathbf{s}[m]|^2 \quad (8.41)$$

15. On page 172, equation (8.76) has a typo; the covariance matrix  $\mathbf{C}_{\mathbf{x}}$  should be  $\mathbf{C}_{\mathbf{s}}$ . The equation should read:

$$\mathbf{K} = \mathbf{C}_{\mathbf{s}} \left( \mathbf{I}_D + \frac{\mathbf{V}^H \mathbf{V} \mathbf{C}_{\mathbf{s}}}{\sigma_n^2} \right)^{-1} \left( \frac{\mathbf{V}^H \mathbf{V} \mathbf{C}_{\mathbf{s}}}{\sigma_n^2} \right) \quad (8.76)$$

16. On page 186, equation (9.3) has a typo; the velocity terms should have a difference operation, not a sum. The equation should read:

$$v_i = (\mathbf{v} - \mathbf{v}_i)^T \frac{(\mathbf{x} - \mathbf{x}_i)}{\|\mathbf{x} - \mathbf{x}_i\|} \quad (9.3)$$

17. On page 211, equations (10.26) and (10.27), we note that our use of the Jacobian does not match other conventions (notably, that in use by Boyd in Convex Optimization. Our Jacobian is the transpose of the one defined therein, and so our expressions for the Fisher Information Matrix are slightly different.

18. On page 221, equation (11.6) has a typo; the entry in the lower-left corner should be  $\sigma_N^2$  instead of  $\sigma_1^2$ . Furthermore, the equation would be easier to



read if the matrix elements were center-justified instead of left-justified. The equation should read:

$$\mathbf{C}_p = c^2 \begin{bmatrix} \sigma_1^2 + \sigma_N^2 & \sigma_N^2 & \cdots & \sigma_N^2 \\ \sigma_N^2 & \sigma_2^2 + \sigma_N^2 & \cdots & \sigma_N^2 \\ \vdots & \vdots & \ddots & \vdots \\ \sigma_N^2 & \sigma_N^2 & \cdots & \sigma_{N-1}^2 + \sigma_N^2 \end{bmatrix} \quad (11.6)$$

19. On page 234, there is a typo in text referring to Figure 11.6(b). The sentence:

*"The same scenario is repeated in Figure 11.6(11.6b) with the addition of a fourth sensor at the origin."*

should read:

*"The same scenario is repeated in Figure 11.6(b) with the addition of a fourth sensor at the origin."*

20. On page 279, equation (13.12) has a type,  $v$  should be  $\nu$ . The equation should read:

$$\mathbf{D}_\nu = \text{diag} \{ \exp(-j\nu \mathbf{m}) \} \quad (13.12)$$

21. On page 291, equation (A.21) and the preceding text, there is a typographical error. The quantity

$$f_{X^\epsilon} \quad (A.21)$$

should be:

$$f_{X^2} \quad (A.21)$$

22. On page 315, figure C.5, there is a typographical error. The label on the vertical axis should read *Zenith Attenuation (linear)*, it erroneously specifies that the attenuation is plotted in dB.